Highly efficient DSB-free base editing for streptomycetes with CRISPR-BEST

Yaojun Tong[a], Christopher M. Whitford[a,b], Helene L. Robertsen[a], Kai Blin[a], Tue S. Jørgensen[a], Andreas K. Klitgaard[a], Tetiana Gren[a], Xinglin Jiang[a], Tilmann Weber[a,1], and Sang Yup Lee[a,c,1]

[a]The Novo Nordisk Foundation Center for Biosustainability, Technical University of Denmark, 2800 Kongens Lyngby, Denmark; [b]Center for Biotechnology (CeBiTec), Bielefeld University, 33615 Bielefeld, Germany; and [c]Metabolic and Biomolecular Engineering National Research Laboratory, Department of Chemical and Biomolecular Engineering (BK21 Plus Program), Center for Systems and Synthetic Biotechnology, Institute for the BioCentury, Korea Advanced Institute of Science and Technology (KAIST), 305-701 Daejeon, Republic of Korea

Contributed by Sang Yup Lee, August 28, 2019 (sent for review August 5, 2019; reviewed by Christophe Corre and Chaitan Khosla)

Streptomycetes serve as major producers of various pharmacologically and industrially important natural products. Although CRISPR-Cas9 systems have been developed for more robust genetic manipulations, concerns of genome instability caused by the DNA double-strand breaks (DSBs) and the toxicity of Cas9 remain. To overcome these limitations, here we report development of the DSB-free, single-nucleotide–resolution genome editing system CRISPR-BEST (CRISPR-Base Editing SysTem), which comprises a cytidine (CRISPR-cBEST) and an adenosine (CRISPR-aBEST) deaminase-based base editor. Specifically targeted by an sgRNA, CRISPR-cBEST can efficiently convert a C:G base pair to a T:A base pair and CRISPR-aBEST can convert an A:T base pair to a G:C base pair within a window of approximately 7 and 6 nucleotides, respectively. CRISPR-BEST was validated and successfully used in different *Streptomyces* species. Particularly in nonmodel actinomycete *Streptomyces collinus* Tü365, CRISPR-cBEST efficiently inactivated the 2 copies of *kirN* gene that are in the duplicated kirromycin biosynthetic pathways simultaneously by STOP codon introduction. Generating such a knockout mutant repeatedly failed using the conventional DSB-based CRISPR-Cas9. An unbiased, genome-wide off-target evaluation indicates the high fidelity and applicability of CRISPR-BEST. Furthermore, the system supports multiplexed editing with a single plasmid by providing a Csy4-based sgRNA processing machinery. To simplify the protospacer identification process, we also updated the CRISPy-web (https://crispy.secondarymetabolites.org), and now it allows designing sgRNAs specifically for CRISPR-BEST applications.

streptomycetes | CRISPR base editor | cytidine deaminase | adenosine deaminase | genome editing

The increasing occurrence of multidrug-resistant pathogens is a global health threat that likely will worsen in the near future (1). One important pillar in counteracting these worrisome developments is to find and develop novel effective antibiotics. Remarkably, more than 70% of our current antibiotics are derived from natural products of streptomycetes. Genome mining (2) indicates that these organisms still possess a huge unexploited potential of producing novel natural products (3). However, for exploiting this potential, modern biotechnologies, such as metabolic engineering or synthetic biology (3, 4), are heavily relying on efficient genetic manipulation or gene editing approaches. Unfortunately, it is difficult to do genome manipulation of actinomycetes, mainly due to their mycelial growth, intrinsic genetic instability, and very GC-rich (>70%) genomes. There are established traditional mutagenesis methods, but they are relatively inefficient and very time- and labor-consuming (5, 6).

Recently, CRISPR-Cas systems, originating from the bacterial adaptive immune systems, have been successfully used for genome editing in a variety of organisms (7). Also for actinomycetes, efficient CRISPR-Cas9 systems were developed to do scarless gene knockout, knockin, and reversible gene knockdown (8–10). Although these systems provide excellent flexibility and high efficiency, severe challenges still remain. In many actinomycetes, the (over) expression of Cas9 has severe toxic effects and leads to a high number of unwanted off-target effects (11, 12). Furthermore, the linear chromosomes show a relatively high intrinsic instability and can tolerate large-scale chromosomal deletions and rearrangements (13). DNA double-strand breaks (DSBs) in the arm regions are considered major triggers of this instability (14) and often co-occur with the DSB-based gene manipulation procedures, like CRISPR-Cas9.

Introduction of DSB-based in-frame deletion/small insertions and deletions (indels) is not the only way to generate a null mutant. Here, we present an alternative highly efficient approach to generate mutations in streptomycetes without the requirement of a DSB. The targeted conversion of cytidine (C) to thymidine (T) can lead to the introduction of stop codons (15–18), while conversion of C to T or adenosine (A) to guanosine (G) can cause loss-of-function mutations of coding genes in different organisms. Such tools are named "base editors." Typically, 2 types of base editors have been reported, cytidine

Significance

Although CRISPR-Cas9 tools dramatically simplified the genetic manipulation of actinomycetes, significant concerns of genome instability caused by the DNA double-strand breaks (DSBs) and common off-target effects remain. To address these concerns, we developed CRISPR-BEST, a DSB-free and high-fidelity single-nucleotide–resolution base editing system for streptomycetes and validated its use by determining editing properties and genome-wide off-target effects. Furthermore, our CRISPR-BEST toolkit supports Csy4-based multiplexing to target multiple genes of interest in parallel. We believe that our CRISPR-BEST approach is a significant improvement over existing genetic manipulation methods to engineer streptomycetes, especially for those strains that cannot be genome-edited using normal DSB-based genome editing systems, such as CRISPR-Cas9.

Author contributions: Y.T. designed research; Y.T., C.M.W., H.L.R., T.S.J., A.K.K., T.G., and X.J. performed research; Y.T., C.M.W., H.L.R., T.S.J., A.K.K., and T.W. analyzed data; K.B. designed the spacer identification software; T.W. and S.Y.L. supervised and steered the project; and Y.T., T.W., and S.Y.L. wrote the paper.

Reviewers: C.C., University of Warwick; and C.K., Stanford University.

The authors declare no competing interest.

Data deposition: All generated data were deposited to the National Center for Biotechnology Information (NCBI) under BioProject accession no. PRJNA557658. The raw data are available in the Sequence Read Archive (SRA) under accession nos. SRR9879387–SRR9879391. The genome assembly, which is *S. coelicolor* NC_003888.3 polished with Illumina MiSeq data from the culture used for experiments, is available under accession no. CP042324.

[1]To whom correspondence may be addressed. Email: tiwe@biosustain.dtu.dk or leesy@kaist.ac.kr.

This article contains supporting information online at www.pnas.org/lookup/suppl/doi:10.1073/pnas.1913493116/-/DCSupplemental.

First published September 23, 2019.

deaminase-based (C to T) and adenosine deaminase-based (A to G) base editors, and the prominent examples are the BE3 system (19) and the ABE7.10 system (20), respectively, for editing human cell lines. BE3 was constructed by artificially fusing of the rat APOBEC1 (rAPOBEC1) cytidine deaminase, a Cas9 nickase (Cas9n), and a uracil glycosylase inhibitor (UGI) (19), while ABE7.10 was established by fusing of the laboratory evolved *Escherichia coli* adenosine deaminase TadA (ecTadA) and a Cas9n (20). Because deamination can only occur in single-strand DNA (ssDNA), both G:C-to-A:T conversion by cytidine deamination and A:T-to-G:C conversion by adenosine deamination are restricted to a small editing window in the R-loop (21) region formed by Cas9n:sgRNA:target DNA recognition without involving a DSB. As the cellular mismatch repair (MMR) machinery prefers to repair the mismatch in a nicked strand (19), we decided to select Cas9n:sgRNA complex as the delivery system for the deaminases.

Here, we report the establishment, validation, genome-wide off-target evaluation, and multiplexed genome editing of the CRISPR base editor system (CRISPR-BEST) in streptomycetes.

Results

The Design of Single-Plasmid–Based CRISPR-BEST for Streptomycetes. In order to address the limitations of CRISPR-Cas9 in streptomycetes, we designed a pSG5-based (22), DSB-free, single base pair editing system termed CRISPR-BEST: CRISPR-Base Editing SysTem (Fig. 1*A*). The "all-in-one-vector" system is available in 2 variants, CRISPR-cBEST (using a cytidine deamination; Addgene plasmid no. 125689) and CRISPR-aBEST (using an adenosine deamination; Addgene plasmid no. 131464). To facilitate the 20-nt spacer cloning step and increase the cloning efficiency, we modified the original sgRNA cassette of pCRISPR-Cas9 (10) to be compatible with single-strand DNA (ssDNA) oligo bridging method (Fig. 1*B* and *SI Appendix, Materials and Methods*). The sgRNA

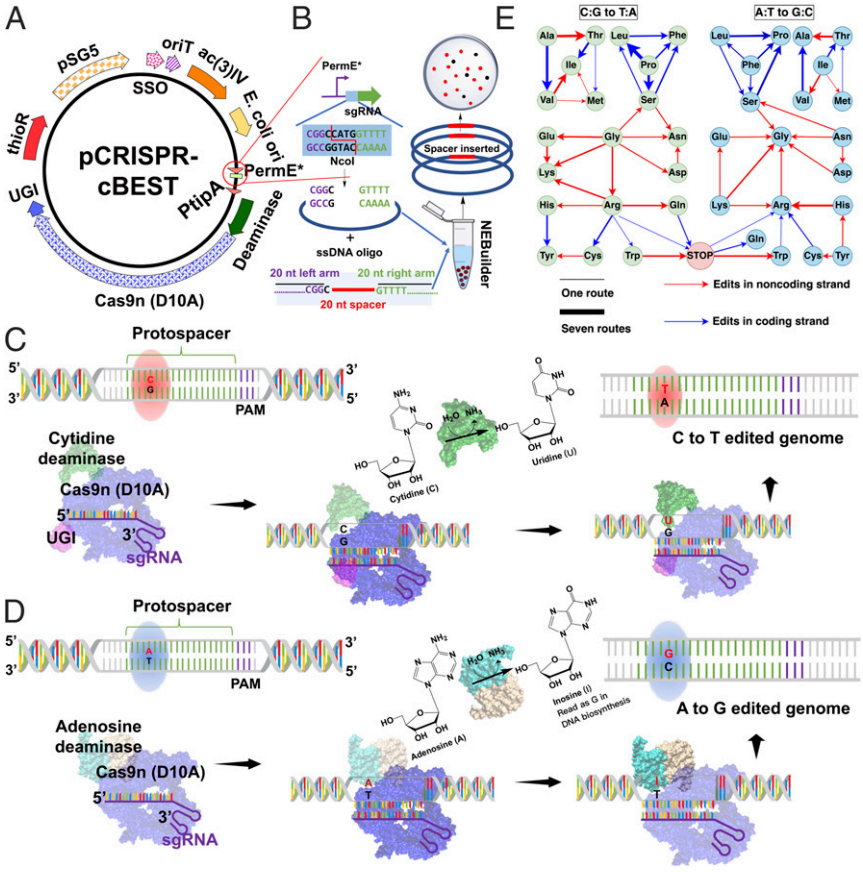

Fig. 1. Rationale and workflow of CRISPR-BEST. (*A*) The CRISPR-BEST plasmid is a pSG5 replicon-based, temperature-sensitive *E. coli–Streptomyces* shuttle plasmid. The displayed plasmid map is CRISPR-cBEST, in which the core component is the fusion protein of *S. coelicolor* A3(2) codon-optimized rAPOBEC1, Cas9n (D10A), and UGI. The key component of CRISPR-aBEST is a fusion protein of *S. coelicolor* A3(2) codon-optimized ecTadA, and Cas9n (D10A). Expression of the fusion proteins is controlled by a promoter PtipA. In our tests, the leakage expression is enough to carry out the base editing functionality; stronger expression can be induced by adding thiostrepton. (*B*) The sgRNA cassette is under control of the promoter PermE*. A PCR-free, 1-step ssDNA bridging approach can be applied for the 20-bp spacer cloning. (*C* and *D*) Overview of the base editing strategies for CRISPR-cBEST and CRISPR-aBEST, respectively. The target nucleotide within the editing window is indicated in red and the possible active domains in each step is shown in a brighter color. First, sgRNA (purple) binds to D10A Cas9n (blue), ending up with Cas9n:sgRNA complex. Second, the Cas9n:sgRNA complex finds and binds its target DNA, which mediates the separation of the double-stranded DNA to form the R-loop structure. Third (*C*), for C-to-T editing, a tethered *Streptomyces*-optimized cytidine deaminase rAPOBEC1 (green) converts the target C in the nontargeted strand to a U by cytidine deamination. Due to the inhibition of the nucleotide excision repair (NER) pathway by UGI, the cellular mismatch repair (MMR) becomes the dominant DNA repair pathway. It preferentially repairs the mismatch in a nicked strand. Therefore, the G in the targeted strand, which is nicked by D10A Cas9n, is going to be efficiently replaced by A and, in the next replication cycle, repaired to a T:A base pair. (*D*) For A-to-G editing, a tethered *Streptomyces*-optimized adenosine deaminase ecTadA heterodimer (cyan-yellow) converts the target A in the nontargeted strand to an I by deamination. As I is read as G by DNA polymerase, the resulting I:T heteroduplex is permanently converted to a G:C base pair during DNA replication. (*E*) Representation of the possible amino acid exchanges resulting from CRISPR-BEST. Blue lines indicate that the edited nucleotide is in the coding strand, while red lines indicate that the edited nucleotide is in the noncoding strand. The thickness of the lines indicates the number of possible routes that can end up with the same amino acid exchange by CRISPR-BEST.

cassette is controlled by a constitutive PermE* promoter. As core components, the gene encoding the cytidine deaminase rAPOBEC1 (GenBank accession no. NM_012907.2) and the adenosine deaminase ecTadA (GenBank accession no. NP_417054.2) were codon-optimized for *Streptomyces* (*SI Appendix*, Fig. S4) and then fused to the N terminus of the *Streptomyces* codon-optimized Cas9n (D10A) (*SI Appendix*, Fig. S4) using a 16- and 32-amino acid flexible linker, respectively. The expression of the fusion protein is driven by the inducible, but leaky, promoter PtipA. The *tipA* promoter requires the presence of the thiostrepton-responsive activator TipA (23), and the TipA encoding gene is widely present in most *Streptomyces* (24). However, it is crucial to confirm the presence of *tipA* in the host genome before use of CRISPR-BEST. Localized by the target binding capability of sgRNA/Cas9n complex, the deamination reaction (Fig. 1 *C* and *D*) takes place in the single-strand DNA within the R-loop structure formed by the annealing of sgRNA and target dsDNA. The deamination of the targeted C in a C:G base pair and the targeted A in an A:T base pair results in a U:G mismatch and an I:T mismatch, respectively (Fig. 1 *C* and *D*), which are wobble base pairs. In DNA replication, U is recognized as T, and I (inosine) is recognized as G. As U is an illegitimate DNA base, it normally will be recognized and then excised by uracil-DNA glycosylases (UDGs) (25). This initiates the conserved nucleotide excision repair (NER) (26), leading to the reversion to the original base pair. However, this process can be inhibited by a UGI (Fig. 1*C*). In CRISPR-cBEST, the *Streptomyces* codon-optimized UGI (*SI Appendix*, Fig. S4) from *Bacillus* phage AR9 (GenBank accession no. YP_009283008) is fused to the C terminus of Cas9n (D10A) using a 4-amino acid flexible linker. Therefore, the inhibition of NER triggers the conserved cellular mismatch repair (MMR) (27) to efficiently convert the wobble base pair U:G to U:A (Fig. 1*C*). However, no similar inhibitor was reported for NER of the I:T mismatch. This could be one of the reasons leading to the lower editing performance of the adenosine deaminase-based base editors. The efficiency of the MMR repair can be increased by introducing a single-strand DNA nick in proximity to the editing site (19). Next, the illegitimate DNA bases will be repaired during DNA synthesis (Fig. 1 *C* and *D*). This process generates permanent modifications of the target DNA without the requirement of a DSB. By clever selection of the target sites, base editors can thus generate point mutations resulting in amino acid replacements or the introduction of STOP codons (Fig. 1*E* and *SI Appendix*, Tables S6 and S7).

CRISPR-cBEST Efficiently Converts the Targeted C into T in *Streptomyces coelicolor*. For a proof of concept, the actinorhodin biosynthetic gene cluster region of *S. coelicolor* A3(2) was selected as a target. Potential protospacers containing the editable cytidines were identified in the genes of the target region using CRISPy-web (28) (https://crispy.secondarymetabolites.org), which we have updated for this study to support sgRNA identification for CRISPR-BEST sgRNA applications. In total, 12 protospacers were selected to construct sgRNAs for validation of CRISPR-cBEST, 6 targeting the coding strand and 6 targeting the noncoding strand.

The reported cytidine deaminase-based base editors have a less than 10-nucleotide editing window in the PAM-distal region regardless of the linker sizes between the deaminase and dCas9/Cas9n (19, 29). Therefore, we investigated all of the cytidines within the hypothetic 10-nucleotide editing window in the PAM-distal position. We observed that not a single cytidine was converted into a thymidine in the first 3 nucleotides of this hypothetic editing window of all 12 protospacers, while C-to-T editing was observed in all other positions (*SI Appendix*, Fig. S1*A*). Thus, the editing window of CRISPR-cBEST was assigned to 7 nucleotides (positions 4 to 10 in the hypothetic editing window) in the PAM-distal region (Fig. 2*A*). Overall, the cytidines in the editing window were converted into thymidines with frequencies between 30% and 100% (*SI Appendix*, Fig. S1*A*). Only in 3 cases, where the C is preceded by a G, was no conversion observed. From these results, we could reason that the sequence context and position of the target C will affect the editing efficiency.

CRISPR-aBEST Can Convert the Targeted A into G in *S. coelicolor*. In parallel with the validation of CRISPR-cBEST, we also selected 2 spacers from the *S. coelicolor* genome, one targeting the coding strand of SCO5087 and the other targeting the noncoding strand of an intergenic region between SCO2181 and SCO2182. Both of the sgRNAs contain adenosines within a hypothetic editing window of 6 nt. We observed that the targeted adenosines were indeed converted to guanosines, albeit with a lower editing efficiency (*SI Appendix*, Fig. S1*B*) compared to CRISPR-cBEST. This observation is consistent with a previous report (20).

Systematic Characterization of CRISPR-cBEST and CRISPR-aBEST In Vivo. For the rAPOBEC1-based cytidine base editor, different performance was reported in vitro and in vivo (19). The sequence context of ecTadA-based adenosine base editor, to our best knowledge, was fully characterized neither in vitro nor in vivo. In order to systematically evaluate the effects of sequence context and the target nucleotide position on editing efficiency in a "close-to-application" context in vivo, we designed a matrix based on the 4 possible NC or NA combinations (with N representing T, A, C, or G) of the target nucleotide with all 4 nucleotides. In the matrix for CRISPR-cBEST, the target C of each NC combination was distributed in all 7 possible positions (Fig. 2*A*). We used PatScanUI (30) to identify the possible protospacer variants in the genome of *S. coelicolor* A3(2). Seven such protospacers in nonessential genes were selected and tested experimentally (Fig. 2*A*). By calculating the C-to-T conversion efficiency (Fig. 2*B*), it became evident that the CRISPR-BEST system is accepting its deamination substrates in the priority of TC > CC > AC > GC (Fig. 2*B*). This finding is consistent with the in vitro results of other reports (19, 31). Within the 7-nucleotide editing window, we observed that positions 2, 3, and 4 showed highest editing efficiency (Fig. 2*B*).

Due to the low AT content of *S. coelicolor*, we could not find all 7 protospacers to form the matrix for CRISPR-aBEST. Only 6 (Fig. 2*C*) of 7 protospacers were identified in the genome of *S. coelicolor* A3(2). By measuring the A-to-G conversion efficiency, we could see that the overall efficiency of A-to-G editing was lower than C-to-T editing (Fig. 2*D*), which is consistent with the results we obtained from our proof-of-concept experiments (*SI Appendix*, Fig. S1). The editing window of CRISPR-aBEST is approximately 6 nt, which is narrower than CRISPR-cBEST (Fig. 2 *B* and *D*). Moreover, only TA and GA combinations showed good editing efficiency in positions 2 through 4 (Fig. 2*D*).

CRISPR-BEST Applications in Amino Acid Substitution of the Model Actinomycete *S. coelicolor*. By converting C to T or A to G in any of the 64 natural codons, 62 different amino acid substitutions can be generated, which cover all 20 natural amino acids as well as 3 STOP codons (Fig. 1*E* and *SI Appendix*, Tables S6 and S7). To validate CRISPR-cBEST on amino acid substitution applications in vivo, 2 genes, SCO5087 (ActIORF1, actinorhodin polyketide beta-ketoacyl synthase subunit alpha, KSα of minimal PKS) and SCO5092 (ActVB, dimerase), from the biosynthetic pathway of the diffusible, blue-pigmented polyketide antibiotic actinorhodin in *S. coelicolor* (Fig. 3*A*) were selected. sgRNAs targeting these 2 genes were designed and cloned into CRISPR-BEST plasmids. Sanger sequencing of the targeted region revealed that all target cytidines were converted to thymidines, ending up with desired amino acid substitutions or STOP codon introductions (Fig. 3 *B*–*F*). The loss of function of the gene encoding ActIORF1 (SCO5087) completely eliminates actinorhodin biosynthesis (Fig. 3*A*) and thus leads to the dark blue-colored phenotype of the colonies under alkaline condition

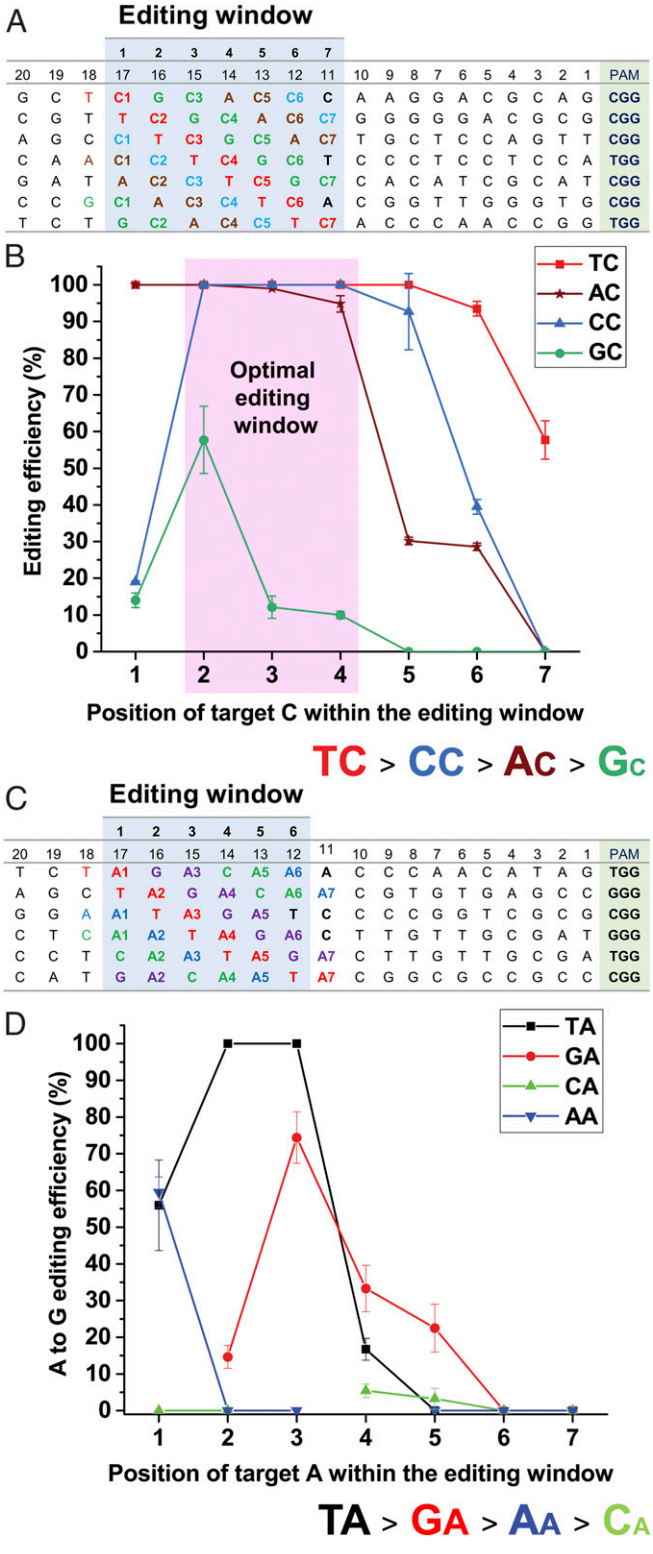

Fig. 2. In vivo systematic characterization of CRISPR-BEST. (*A* and *C*) Positional effect of each NC and NA combination on editing efficiency in vivo. Matrixes of TCGCACC and TAGACAA were designed to investigate the optimal NC and NA combination and target C and target A position within the editing window, respectively. Protospacer (20 nt) and its PAM was displayed. The editing window was masked in light blue. (*B* and *D*) Each NC and NA combination was varied from positions 1 to 7 within the protospacer. The target regions of 10 to 20 CRISPR-BEST–treated exconjugants of each protospacer were PCR-amplified and Sanger-sequenced. For mixed trace signals, the secondary peak calling function of CLC Main Workbench 8 (QIAGEN Bioinformatics) was applied to calculate the editing efficiency. The 3-nt window in pink showed the optimal editing efficiency of CRISPR-cBEST. Values and error bars are the mean and SD of 2 to 3 independent conjugations using the same pCRISPR-BEST plasmids.

(Fig. 3*B*). ActVB (SCO5092) is one of the key enzymes that are required for the dimerization of 2 polyketide precursors as one of the last steps of the actinorhodin biosynthesis (Fig. 3*A*). A null mutant by a STOP codon introduction (Fig. 3*F*) in this gene leads to the accumulation of the intermediate dihydrokalifungin (DHK; Fig. 3*A*). Compared to actinorhodin, the colonies exhibit brownish color on ISP2 agar plate (alkaline condition; Fig. 3*B*). In all 4 tested cases, the targeted C was converted to T with an editing efficiency of nearly 100% (*SI Appendix*, Fig. S2).

Genome-Wide Off-Target Evaluation of CRISPR-BEST. Off-target effects have been observed in applications of both cytidine and adenosine base editors (32, 33). In order to systematically evaluate the off-targets of our CRISPR-BEST in streptomycetes, we applied a genome-wide SNP (single nucleotide polymorphism) profiling approach to analyze 2 randomly selected CRISPR-cBEST–edited *S. coelicolor* strains with sgRNA SCO5087-1 and sgRNA SCO5092, respectively (Fig. 3*C* and *SI Appendix*, Table S4), and 2 randomly selected CRISPR-aBEST–edited *S. coelicolor* strains with sgRNA ABE_matrix_2 and sgRNA ABE_matrix_3, respectively (Fig. 2*C* and *SI Appendix*, Table S4) (34). A single Illumina MiSeq 2 × 150-nt run yielded between 3,133,656 and 4,407,008 reads per sample, corresponding to coverages between 54 and 69. Single nucleotide insertions and deletion were primarily observed in both WT and edited strains in the homopolymer genomic regions, particularly in poly-G and poly-C regions, which are notoriously difficult to correctly assemble, a known limitation in the breseq error model (35). As the *S. coelicolor* WT strain we maintained in laboratory (*S. coelicolor* WT_{NBC}, strain CFB_NBC_0001; *SI Appendix*, Table S2) has already accumulated nearly 100 SNPs (10) against the reference sequence NC_003888 (36), and because the SNPs likely accumulate over time, we also included our *S. coelicolor* WT_{NBC} in the sequencing and then used its data to polish the NC_003888 sequence, ending up with NC_003888.3NBC. We could still observe a background SNP profile of 29 SNPs in the *S. coelicolor* WT_{NBC} strain we used in this study, which could be caused by low-frequency variants (Fig. 4*A*). We reasoned that mapping the Illumina MiSeq reads of each sequenced strain to the polished reference genome sequence NC_003888.3NBC allows a more precise off-target evaluation for CRISPR-BEST. The potential off-target SNPs were obtained by subtracting the desired SNPs from the total SNPs. In general, the number of the potential off-target SNPs was small: 56, 38, 33, and 27 SNPs were identified from strains bearing sgRNA SCO5087-1, sgRNA SCO5092, sgRNA ABE_matrix_2, and sgRNA ABE_matrix_3, respectively (Fig. 4 *B*–*E*). As expected, the C-to-T and A-to-G changes were the dominant off-target effect of cytidine base editor CRISPR-cBEST (Fig. 4 *B* and *C*), with the proportions of 45% and 48% over total SNPs of strains with sgRNA SCO5087-1 and sgRNA SCO5092, respectively. There was a very similar pattern of SNP profiles caused by the adenosine base editor CRISPR-aBEST and the background, the WT used in this study, indicating a negligible off-target effect of CRISPR-aBEST (Fig. 4 *A*, *D*, and *E*). Our results showing higher off-target effects caused by the cytidine deaminase-based base editor CRISPR-cBEST than the adenosine deaminase-based base editor CRISPR-aBEST are consistent with a similar case study in rice (33). As only those SNPs within a coding region that cause amino acid substitutions will show potential phenotypic changes, we reasoned that these SNPs might have more biological sense and are worth further investigation. By locating each SNP into the genome, we got an even smaller number of meaningful

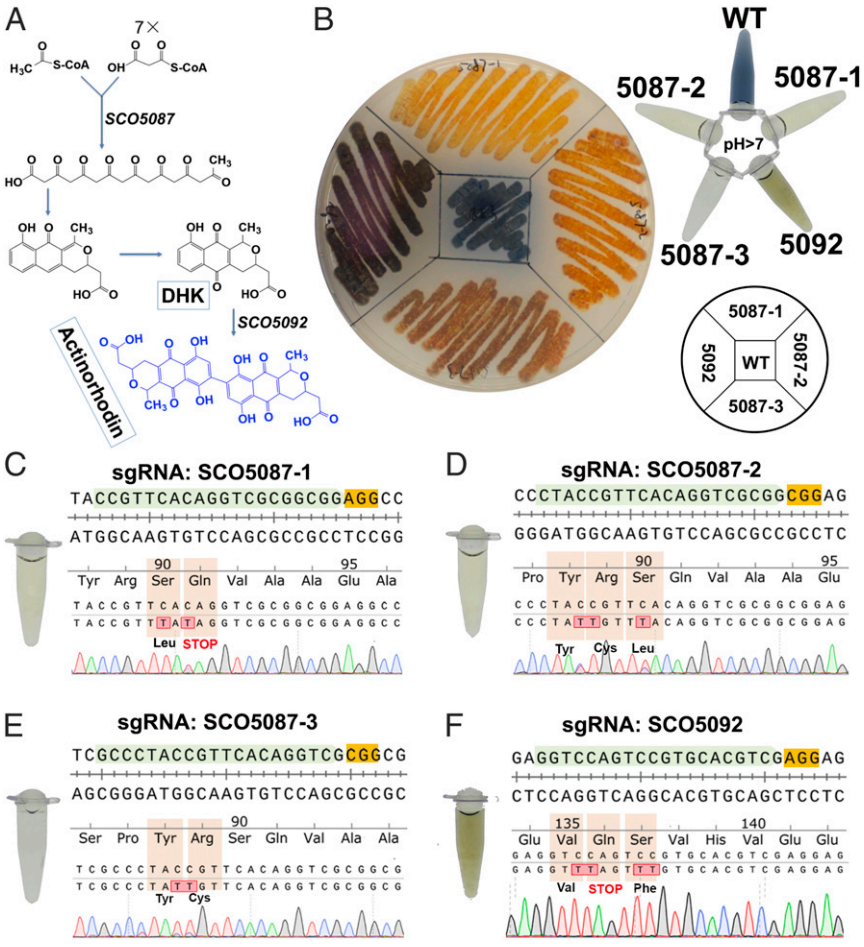

Fig. 3. Applications of CRISPR-cBEST in model actinomycetes *S. coelicolor*. (*A*) A simplified biosynthetic route of the blue-pigmented polyketide antibiotic actinorhodin. SCO5087, coding for the actinorhodin polyketide beta-ketoacyl synthase subunit alpha, and SCO5092, involved in dimerization, were selected as editing targets. (*B*) One *S. coelicolor* A3(2) WT, 3 base-edited SCO5087 mutants (ΔSCO5087 [Q91*], SCO5087 [R89C, S90L], and SCO5087 [R89C]), and 1 base-edited SCO5092 mutant (ΔSCO5092 [Q136*]) were streaked onto ISP2 agar plate (pH > 7) with apramycin. The same corresponding extracts were shown as well. (*C*–*F*) Sanger sequencing traces of the region containing a protospacer together with its PAM are displayed. Protospacers are highlighted in light green, PAM sequences in yellow, and the codons and corresponding amino acids are indicated. Detailed editing efficiency is shown in *SI Appendix*, Fig. S2*A*.

amino acid changes caused by SNPs (Fig. 4*F*). Notably, we identified 18 meaningful amino acid changes in the WT we used in this study (Fig. 4*F*). For the 2 CRISPR-cBEST–edited strains, we saw 34 and 24 meaningful amino acid changes, while, for the 2 CRISPR-aBEST–edited strains, we observed 21 and 20 meaningful amino acid changes (Fig. 4*F*). The results we got from the genome-wide off-target evaluation indicates that our CRISPR-BEST is a relatively high-fidelity genome-editing system for streptomycetes.

CRISPR-cBEST Applications in the Nonmodel Streptomycete *Streptomyces griseofuscus*. As a specific application of CRISPR-BEST, the rational introduction of stop codons into genes has great potential in gene inactivation. By converting a C:G pair to a T:A pair by CRISPR-cBEST, Arg codons (**C**GA), Gln codons (**C**AA and **C**AG), and Trp codons (T**GG**, target C in noncoding strand) can be changed to STOP codons (TGA, TAA, and TAG; Fig. 1*E* and *SI Appendix*, Table S6). For generalizing this strategy, we systematically analyzed the number of potential target sites that can lead to a STOP codon introduction into the nonessential secondary metabolites biosynthesis genes of *S. coelicolor* A3(2), *Streptomyces collinus* Tü365, and *S. griseofuscus* DSM40191 using the "STOP mutations" function of the updated CRISPy-web (*SI Appendix*, Fig. S5). An average of approximately 13, 14, and 13 possible target sites per gene were identified for *S. coelicolor* A3(2), *S. collinus* Tü365, and *S. griseofuscus* DSM40191, respectively (*SI Appendix*, Tables S8–S10).

To demonstrate the versatility of CRISPR-BEST, we next aimed to use it on several nonmodel streptomycetes. *S. griseofuscus* is a fast-growing strain with an incomplete DNA restriction modification system (37). In the 1980s, it was reported that *S. griseofuscus* accepts external plasmids encoding antibiotic-resistance markers (38–40). However, to the best of our knowledge, manipulations of the genome of the strain have not yet been reported. In order to test our CRISPR-BEST system, we first sequenced the complete genome of *S. griseofuscus* DSM40191. A total of 34 BGCs were predicted by antiSMASH5 (41), from which we picked 4 representative BGCs (*SI Appendix*, Table S11), a hybrid of Nonribosomal peptide synthetase (NRPS)-type 1 polyketide synthase (T1PKS), an NRPS, a hybrid of T1PKS-T3PKS, and a lanthipeptide for demonstration. The key enzyme from each BGC was selected for inactivation by introducing STOP codons in the beginning or central regions of the genes. As expected, STOP codons were precisely introduced into the designed DNA locations with high frequency (60 to 100%; Fig. 5). In comparison with homologous recombination-based gene deletion, the current

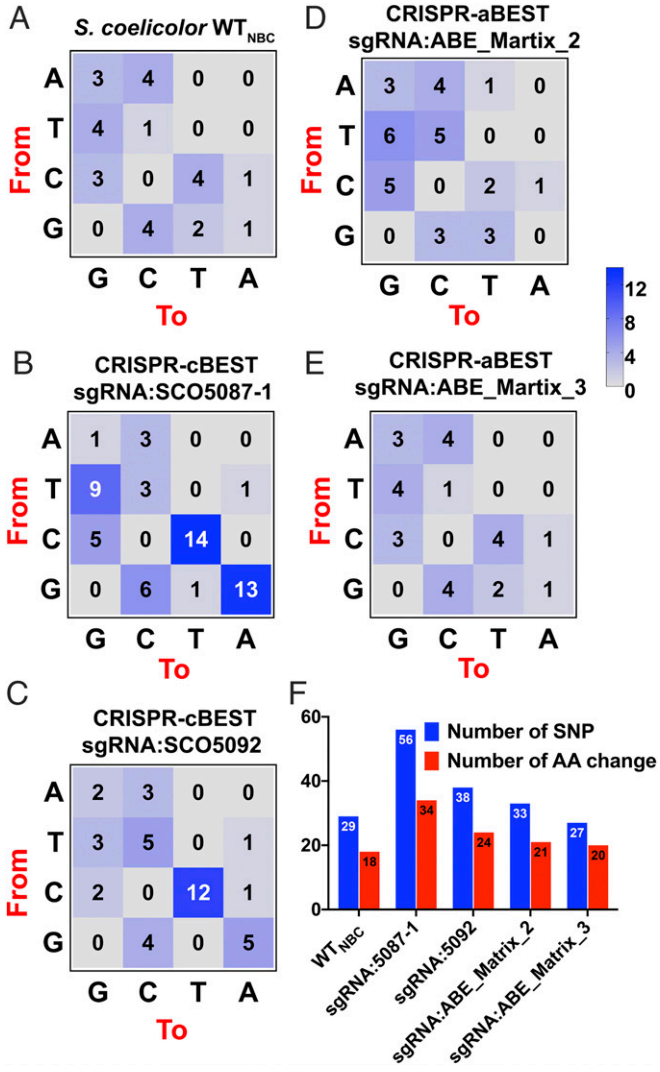

Fig. 4. Genome-wide off-target evaluation of CRISPR-BEST. (*A*–*E*) Distribution of the nucleotide changes of the full genome-sequenced strains against the *S. coelicolor* reference genome sequence NC_003888.3NBC that was polished by the *S. coelicolor* WT_{NBC} strain used in this study. The number in each cell indicates the actual number of certain nucleotide changes outside of the targeted protospacers. (*F*) The bar chart displays the numbers of the meaningful amino acid changes caused by the nucleotide changes from *A* to *E*.

STOP codon introduction protocol saves a lot of time and labor in the cloning of the editing templates (33).

CRISPR-cBEST Can Efficiently Mutate 2 Identical Copies of *kirN* Simultaneously. To include a more difficult "real-world" example, we next elucidated if CRISPR-BEST is capable of simultaneously inactivating 2 identical gene copies of the gene *kirN* (locus B446_01590 and B446_33700) in the duplicated kirromycin biosynthetic gene clusters (BGCs) (42) of the nonmodel actinomycete strain *S. collinus* Tü365 (Fig. 6*A*). Kirromycin is a narrow-spectrum antibiotic first identified in 1972 (43). Its biosynthesis requires an 82-kb gene cluster containing more than 28 genes (42, 44). Within the kirromycin BGC, *kirN* codes for an enzyme that is very similar to the primary metabolism crotonyl-CoA reductase/carboxylases (CCR) (45, 46), and thus it is speculated to be involved in enhancing the pool of ethylmalonyl-CoA, one essential building block of kirromycin. It was shown that the promiscuity of KirCII, the acyltransferase responsible for loading ethylmalonyl-CoA to the PKS assembly line, can be exploited to produce nonnatural kirromycin derivatives, such as allyl- or propargyl kirromycin (45). Thus, it is highly desirable to engineer a strain with lower ethylmalonyl-CoA levels as this may shift the production toward the nonnatural derivatives. We speculate that this could be achieved by the deletion of the BGC-encoded *kirN* gene, which subsequently should reduce the amount of wild-type kirromycin production (46). When using the classical CRISPR-Cas9 system (10) (Fig. 6*B*), all clones obtained after pCRISPR-Cas9 treatment targeting *kirN* completely lost kirromycin production (Fig. 6*C*). Further investigation revealed that the complete loss of kirromycin production and unsuccessful complementation with plasmid-encoded *kirN* was due to large deletions of both chromosome arms (787,795 bp from the left arm and 630,478 bp from the right arm), which contain the 2 copies of the kirromycin BGC (Fig. 6*D*). These deletions were likely caused by the simultaneous DSBs introduced by Cas9.

By using the updated version of CRISPy-web, a protospacer within *kirN* was identified that should introduce an early STOP codon (Fig. 6*E*). After transferring the CRISPR-BEST plasmid with this *kirN*-targeting sgRNA into *S. collinus* Tü365, Sanger sequencing of PCR products of the target region demonstrated that the targeted cytidines were converted to thymidines and thus a STOP codon was successfully incorporated into *kirN* (Fig. 6*E*). The successful amplification of target region and the sharp Sanger sequencing trace signals (Fig. 6*E*) indicated that no fragment was deleted as in CRISPR-Cas9, and 2 copies of the target were edited simultaneously. In the bioactivity assay using the $kirN_{W135*}$ mutant, judging by the sizes of inhibition zone, we could see that kirromycin was still produced but with a much lower yield compared to the wild-type strain (WT; Fig. 6*F*), which was confirmed by LC-MS (Fig. 6*G*). These results are consistent with our previous observation of the *kirN* mutant that was generated by classic homologous recombination-based gene knockout approach (46).

Csy4-Based Multiplexed Editing with a Single CRISPR-cBEST Plasmid. Given the complexity of cellular processes in living organisms, such as the biosynthesis of secondary metabolites, multiple genes often need to be intensively engineered simultaneously within a biosynthetic pathway for both basic and applied studies. CRISPR-based genome editing approaches greatly facilitated the process of strain engineering of streptomycetes (11, 12). However, the multiplexing applications are still limited by the efficacy of sgRNA processing (8, 9). The current sgRNA multiplexing systems (8, 9) for streptomycetes require independent promoter and terminator for each individual sgRNA, which has several drawbacks. For example, multiple use of the same promotor/terminator to control sgRNA transcription may cause plasmid instability due to repetitive sequences; using different promotors/terminators to avoid the instability then raises the concern of unevenly distributed sgRNAs due to the different promoter strengths. To address the aforementioned disadvantages, we designed a Golden Gate Assembly-compatible, Csy4-based [also known as type I-F CRISPR-associated endoribonuclease Cas6 (47); GenBank accession no. PHP80843.1] sgRNA self-processing system, which only requires 1 single promoter and terminator for multiple sgRNAs separated by the Csy4 recognition sites (Fig. 7*A*). To validate the Csy4-based sgRNA multiplexing system, we designed a 3-spacer sgRNA array (Fig. 7*A*), which simultaneously targets 3 key enzymes from 3 BGCs in *S. coelicolor*: SCO5087 from the actinorhodin gene cluster, SCO3230 from the CDA (calcium-dependent antibiotic) gene cluster, and SCO5892 from the (RED) undecylprodigiosin gene cluster (Fig. 7*A*). After editing, we could clearly see that both blue and red pigments were clearly disappeared in most of the picked exconjugants (Fig. 7*B* and *SI Appendix*, Fig. S6). Sanger sequencing

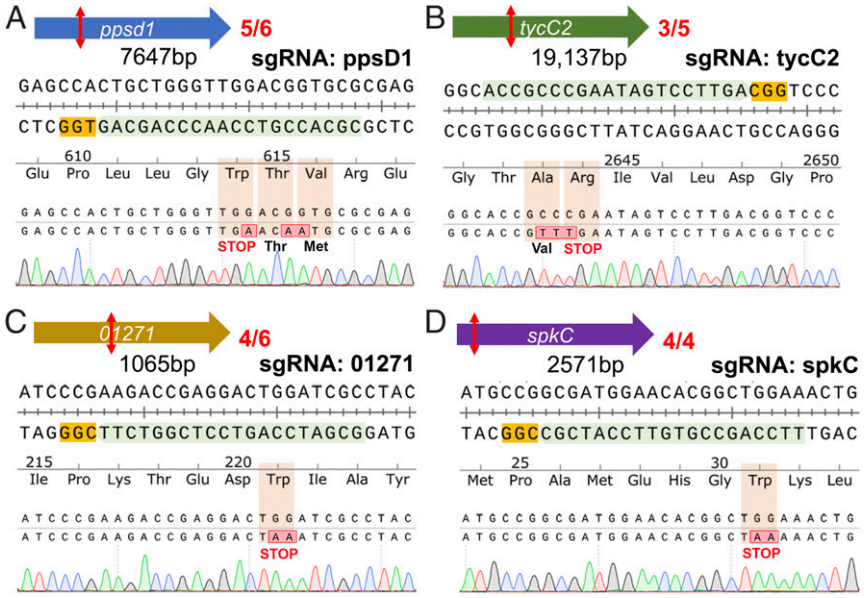

Fig. 5. CRISPR-cBEST application of STOP codon introduction in nonmodel actinomycete *S. griseofuscus*. Sanger sequencing traces of the region containing a protospacer together with its PAM of the 4 selected core biosynthetic genes are displayed. Protospacers are highlighted in light green, PAM sequences in yellow, and the codons and corresponding amino acids are indicated. The number in red represents randomly picked exconjugants of "successful STOP codon introduction clones/total sequenced clones." The gene size is marked. The red double-headed arrow represents the position of STOP codon introduced. (*A*) ppsd1 gene of the NRPS-T1PKS BGC. (*B*) *tycC2* gene of the NRPS BGC. (*C*) *01271* gene of the T1PKS-T3PKS BGC. (*D*) spkC gene of the lanthipeptide BGC.

confirmed that both SCO5087 and SCO5892 were 100% edited as designed (Fig. 7 *C* and *E*), while the editing efficiency of SCO3230 was less than half that of SCO5087 and SCO5892 (Fig. 7*D*).

Discussion

Genome mining of actinobacterial, and especially streptomycetes, genomes revealed a huge untapped potential for the biosynthesis of novel natural products (48). Despite the remarkable knowledge of novel biosynthetic pathways in streptomycetes (3), the limited methods and tools to access, manipulate, and metabolically engineer those genomes heavily restricts the discovery of novel bioactive natural products in streptomycetes. Modern drug development heavily relies on advanced biotechnology, especially genetic manipulation means, which are required by systems and synthetic biology and metabolic engineering. However, compared to other model organisms like *E. coli* and *Saccharomyces cerevisiae*, the available approaches for manipulating the genomes of actinomycetes are relatively limited and normally very time- and labor-consuming.

During the past 3 y, several CRISPR-Cas9–based genome editing systems have been developed with sharply increased efficiency (11, 12). All these methods for generating mutants with CRISPR-Cas9 have in common that 1 or 2 double-strand DNA breaks (DSBs) are introduced at the target locus first, and then the DSB(s) are repaired via the different DSB repair pathways to achieve genome editing events. Even though these CRISPR-Cas9–based approaches have much higher efficiencies than the conventional genetic manipulation protocols (8–10), several major challenges still remain. Precise deletions in bacteria, including actinomycetes, relies on homologous recombination with specifically designed recombination templates. To clone such editing templates from a GC-rich genomic DNA adds time and resources to the genome editing process (11, 12). While the Cas9 toxicity somehow can be addressed by the Cas9 expression/promoter system and the off-target effects by sophisticated sgRNA design algorithms or optimized Cas9 variants, the big challenge of genome instability that leads to undesired deletions or large-scale genome rearrangements remains (13, 14).

In order to address to this, we implemented highly efficient CRISPR/deaminase-mediated base editors, CRISPR-BEST for streptomycetes, which contains both C-to-T (CRISPR-cBEST) and A-to-G (CRISPR-aBEST) base editors. It is an easy to use and highly efficient genome editing system with single-base pair resolution. By the time of designing our base editor system, 2 dCas9- and/or Cas9n- (D10A) mediated cytidine-to-thymidine base editors, BE3 (19) and Target-AID (29), and 1 adenosine-to-guanosine base editor, ABE7.10, were reported. However, Cas9n (D10A) was reported too toxic to be used as the carrier protein of deaminase in *E. coli*, probably because *E. coli* lacks sufficient DNA repair pathways (18). Streptomycetes, however, seem to have more sophisticated DNA error surveillance mechanisms (49). According to our data, Cas9n (D10A) performed almost the same as dCas9 in *S. coelicolor* (*SI Appendix*, Fig. S3). Taking the aforementioned factors into consideration, we decided to use Cas9n as the deaminase delivery vehicle in our CRISPR-BEST system. Instead of characterizing the system in vitro (19), we carried out all characterizations in vivo for both C-to-T and A-to-G base editors, which is much closer to the real-world applications. Results demonstrated that CRISPR-cBEST prefers to take **TC** over other **NC** combinations as its editing substrate, in accordance with other reports (19, 31). We observed almost no editing of the target C in the GC combination, which could be due to the DNA methylation (50). CRISPR-aBEST prefers to take **TA** over other **NC** combinations as its editing substrate.

In a direct comparison between CRISPR-BEST and CRISPR-(d)Cas9 (*SI Appendix*, Table S1), we could clearly see the advantages of CRISPR-BEST. We demonstrated that CRISPR-BEST can be successfully used in difficult cases in which generating similar mutations with CRISPR-Cas9 was unsuccessful (Fig. 6 *A*–*D*). Off-target effects are one of the most critical concerns of all CRISPR-related genome editing systems, especially for the DSB-based CRISPR-Cas9 system.

In order to systematically assess the impact of off-target effects due to the use of CRISPR-cBEST and CRISPR-aBEST, we carried out an unbiased, genome-wide SNP profiling. Very mild

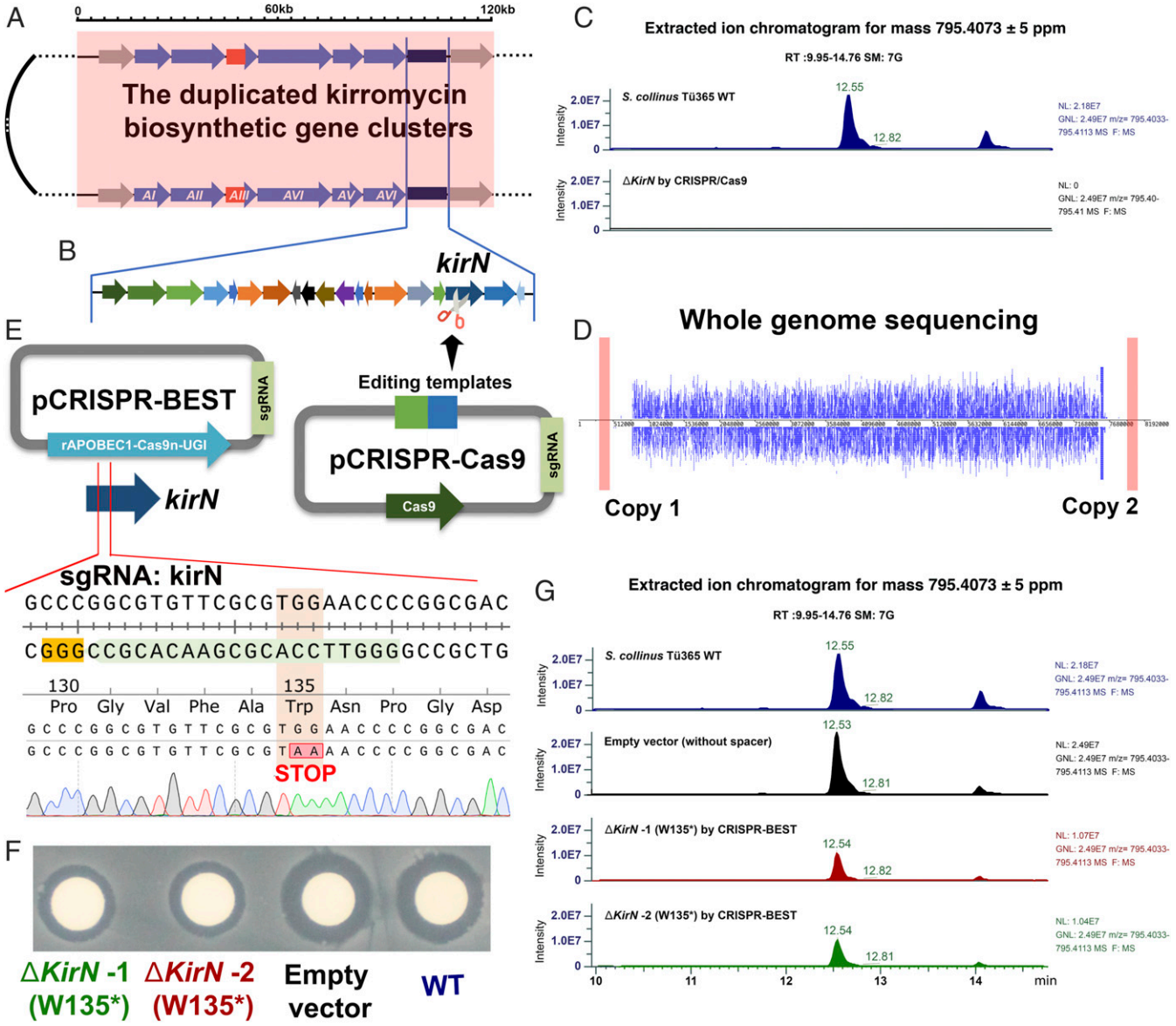

Fig. 6. Applications of CRISPR-cBEST in nonmodel actinomycetes *S. collinus*. (*A*) Schematic representation of the linear chromosome of *S. collinus* Tü365, in which 2 copies of 82-kb-long kirromycin biosynthetic gene cluster (BGC) located ∼341 kb from the left and 422 kb from the right end of the chromosome are shown (42, 45, 46). Within the kirromycin BGC, *kirN* codes an enzyme that is very similar to primary metabolism CCR crotonyl-CoA reductase/carboxylases (CCR) (45, 46), and thus it is speculated to be involved in enhancing the pool of ethylmalonyl-CoA, one building block of kirromycin. A key module containing the *kirN* gene was zoomed in as indicated in the upper part of *B*. (*B*) CRISPR-Cas9–based homologous recombination approach was used to generate an in-frame Δ*kirN* mutant. (*C*) UV-Vis profiles of extracts of WT *S. collinus* Tü365 and Δ*kirN*-Cas9. (*D*) Paired-stack view of Illumina MiSeq reads of the Δ*kirN*-Cas9 mutant (generated by CRISPR-Cas9) mapped against the reference genome of *S. collinus* Tü365. Mapping results showed that both kirromycin clusters encoded near the chromosome ends were lost. The deletion comprises 787,795 bp from the left end and 630,478 bp from the right end. (*E*) CRISPR-cBEST was used to generate *kirN*-null mutant by a STOP codon introduction. Validation of the correct editing of $kirN_{W135*}$ by Sanger sequencing of the PCR-amplified target region. (*F*) Bioactivity testing of 4 extracts from WT, empty vector (no spacer), and 2 independent clones of CRISPR-cBEST–edited $kirN_{W135*}$ using *Bacillus subtilis* 168 as the indicator strain. (*G*) UV-Vis profiles of extracts of the 4 strains used in *F*.

off-target effects were observed for CRISPR-cBEST, with only 20 to 30 meaningful amino acid changes among all of the SNPs potentially caused by the base editors (Fig. 4 *B*, *C*, and *F*). Noticeably, we also observed 29 SNPs in the nontreated parental strain, of which 18 cause amino acid changes (Fig. 4 *A* and *F*). While CRISPR-aBEST demonstrated lower editing efficiency than CRISPR-cBEST (Fig. 2), the potential off-target effects also decreased to a negligible level (Fig. 4 *D* and *E*). All of the off-target results we obtained are sufficiently low such that CRISPR-BEST is useful for broad applications of genome editing in *Streptomyces*.

In order to expand the application of CRISPR-BEST, we established a Csy4-based sgRNA multiplexing system. It can self-process the sgRNA array with many advantages over the current individual independent transcription cassette-based sgRNA multiplexing approaches (8, 9).

In summary, the results we presented here indicated that CRISPR-BEST can achieve highly efficient genome editing with a single-base pair resolution without requiring a DSB. Thus, it reduces the DSB stress on the chromosome and the Cas9 toxicity. We believe that CRISPR-BEST will have huge potential for applications besides inactivating a gene by introducing a stop codon,

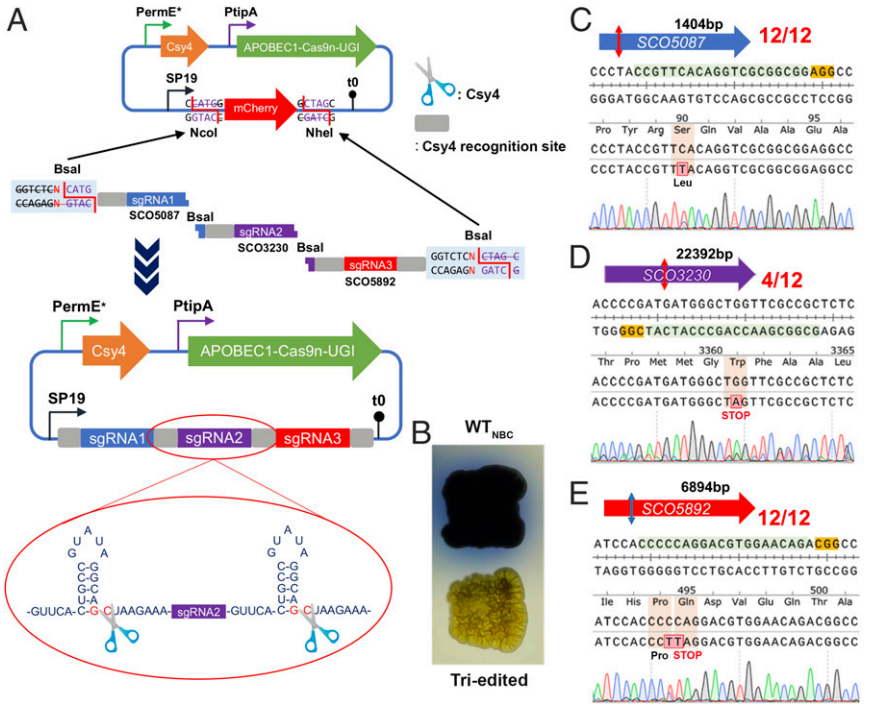

Fig. 7. Csy4-based sgRNA multiplexing applications of CRISPR-cBEST in *S. coelicolor*. (*A*) Schematic representation of the Golden Gate Assembly-compatible, Csy4-based sgRNA multiplexing design. A trisgRNA plasmid containing sgRNAs target SCO5087, SCO3230, and SCO5892 was displayed as an example. (*B*) A phenotypical comparison of the triprotospacer-edited strain with the nonedited wild type *S. coelicolor* strain. (*C–E*) Sanger sequencing traces of the region containing a protospacer together with its PAM of the 4 selected core biosynthetic genes are displayed: (*C*) SCO5087, (*D*) SCO3230, and (*E*) SCO5892. Protospacers are highlighted in light green, PAM sequences in yellow, and the codons and corresponding amino acids are indicated. The number in red represents randomly picked exconjugants of "successful base edited clones/total sequenced clones." The gene size is marked. The double-headed arrow represents the position of protospacer.

such as correcting undesired point mutations or reverting pseudogenes into functional state, protein engineering by exchanging key residues in vivo, and entire pathway engineering by multiplexing sgRNAs in one construct. Taken together, CRISPR-BEST is a powerful addition to the streptomycetes CRISPR-Cas9–based genome editing toolbox.

Materials and Methods

All materials and methods in this study are detailed in *SI Appendix, Materials and Methods*: strains, plasmids, and culture conditions; DNA manipulation; construction of CRISPR-BEST plasmids; construction of the multiplexing CRISPR-cBEST plasmid; single-strand DNA-based PCR-free spacer cloning protocol; in vivo spacer-matrix design using PatScan; CRISPR-BEST support in CRISPy-web; CRISPR-cBEST–compatible protospacers identification using CRISPy-web; in-frame deletion of *kirN* using CRISPR-Cas9–based homologous recombination strategy; validating base pair changes by Sanger sequencing; genome-wide off-target identification of CRISPR-BEST in streptomycetes; Illumina whole-genome sequencing and analysis of *S. collinus* strains; kirromycin fermentation and chemical analysis; bioactivity assay of kirromycin; and assay for actinorhodin extraction.

ACKNOWLEDGMENTS. This work was supported by Novo Nordisk Foundation Grants NNF10CC1016517, NNF15OC0016226, and NNF16OC0021746. S.Y.L. was also supported by the Technology Development Program to Solve Climate Changes on Systems Metabolic Engineering for Biorefineries (NRF-2012M1A2A2026556 and NRF-2012M1A2A2026557) from the Ministry of Science and ICT through the National Research Foundation (NRF) of Korea.

1. G. D. Wright, Solving the antibiotic crisis. *ACS Infect. Dis.* **1**, 80–84 (2015).
2. K. Blin *et al.*, antiSMASH 4.0-improvements in chemistry prediction and gene cluster boundary identification. *Nucleic Acids Res.* **45**, W36–W41 (2017).
3. T. Weber *et al.*, Metabolic engineering of antibiotic factories: New tools for antibiotic production in actinomycetes. *Trends Biotechnol.* **33**, 15–26 (2015).
4. K. S. Hwang, H. U. Kim, P. Charusanti, B. O. Palsson, S. Y. Lee, Systems biology and biotechnology of *Streptomyces* species for the production of secondary metabolites. *Biotechnol. Adv.* **32**, 255–268 (2014).
5. B. Gust, G. L. Challis, K. Fowler, T. Kieser, K. F. Chater, PCR-targeted *Streptomyces* gene replacement identifies a protein domain needed for biosynthesis of the sesquiterpene soil odor geosmin. *Proc. Natl. Acad. Sci. U.S.A.* **100**, 1541–1546 (2003).
6. T. Kieser, M. Bibb, M. Buttner, K. Chater, D. Hopwood, *Practical Streptomyces Genetics* (The John Innes Foundation, Norwich, 2000).
7. J. D. Sander, J. K. Joung, CRISPR-Cas systems for editing, regulating and targeting genomes. *Nat. Biotechnol.* **32**, 347–355 (2014).
8. R. E. Cobb, Y. Wang, H. Zhao, High-efficiency multiplex genome editing of *Streptomyces* species using an engineered CRISPR/Cas system. *ACS Synth. Biol.* **4**, 723–728 (2015).
9. H. Huang, G. S. Zheng, W. H. Jiang, H. F. Hu, Y. H. Lu, One-step high-efficiency CRISPR/Cas9-mediated genome editing in Streptomyces. *Acta Biochim. Biophys. Sin. (Shanghai)* **47**, 231–243 (2015).
10. Y. Tong, P. Charusanti, L. Zhang, T. Weber, S. Y. Lee, CRISPR-Cas9 based engineering of actinomycetal genomes. *ACS Synth. Biol.* **4**, 1020–1029 (2015).
11. Y. Tong, T. Weber, S. Y. Lee, CRISPR/Cas-based genome engineering in natural product discovery. *Nat. Prod. Rep.*, 10.1039/c8np00089a (2018).
12. F. Alberti, C. Corre, Editing streptomycete genomes in the CRISPR/Cas9 age. *Nat. Prod. Rep.*, 10.1039/c8np00081f (2019).
13. J. N. Volff, J. Altenbuchner, Genetic instability of the *Streptomyces* chromosome. *Mol. Microbiol.* **27**, 239–246 (1998).
14. G. Hoff, C. Bertrand, E. Piotrowski, A. Thibessard, P. Leblond, Genome plasticity is governed by double strand break DNA repair in *Streptomyces*. *Sci. Rep.* **8**, 5272 (2018).
15. Y. Wang *et al.*, MACBETH: Multiplex automated *Corynebacterium glutamicum* base editing method. *Metab. Eng.* **47**, 200–210 (2018).
16. C. Kuscu *et al.*, CRISPR-STOP: Gene silencing through base-editing-induced nonsense mutations. *Nat. Methods* **14**, 710–712 (2017).
17. P. Billon *et al.*, CRISPR-mediated base editing enables efficient disruption of eukaryotic genes through induction of STOP codons. *Mol. Cell* **67**, 1068–1079.e4 (2017).
18. S. Banno, K. Nishida, T. Arazoe, H. Mitsunobu, A. Kondo, Deaminase-mediated multiplex genome editing in *Escherichia coli*. *Nat. Microbiol.* **3**, 423–429 (2018).
19. A. C. Komor, Y. B. Kim, M. S. Packer, J. A. Zuris, D. R. Liu, Programmable editing of a target base in genomic DNA without double-stranded DNA cleavage. *Nature* **533**, 420–424 (2016).
20. N. M. Gaudelli *et al.*, Programmable base editing of A•T to G•C in genomic DNA without DNA cleavage. *Nature* **551**, 464–471 (2017).

21. F. Jiang *et al*., Structures of a CRISPR-Cas9 R-loop complex primed for DNA cleavage. *Science* **351**, 867–871 (2016).
22. G. Muth, The pSG5-based thermosensitive vector family for genome editing and gene expression in actinomycetes. *Appl. Microbiol. Biotechnol.* **102**, 9067–9080 (2018).
23. T. Murakami, T. G. Holt, C. J. Thompson, Thiostrepton-induced gene expression in *Streptomyces lividans*. *J. Bacteriol.* **171**, 1459–1466 (1989).
24. B. S. Yun, T. Hidaka, T. Kuzuyama, H. Seto, Thiopeptide non-producing Streptomyces species carry the tipA gene: A clue to its function. *J. Antibiot. (Tokyo)* **54**, 375–378 (2001).
25. N. Schormann, R. Ricciardi, D. Chattopadhyay, Uracil-DNA glycosylases-structural and functional perspectives on an essential family of DNA repair enzymes. *Protein Sci.* **23**, 1667–1685 (2014).
26. B. Van Houten, D. L. Croteau, M. J. DellaVecchia, H. Wang, C. Kisker, 'Close-fitting sleeves': DNA damage recognition by the UvrABC nuclease system. *Mutat. Res.* **577**, 92–117 (2005).
27. J. A. Eisen, P. C. Hanawalt, A phylogenomic study of DNA repair genes, proteins, and processes. *Mutat. Res.* **435**, 171–213 (1999).
28. K. Blin, L. E. Pedersen, T. Weber, S. Y. Lee, CRISPy-web: An online resource to design sgRNAs for CRISPR applications. *Synth. Syst. Biotechnol.* **1**, 118–121 (2016).
29. K. Nishida *et al*., Targeted nucleotide editing using hybrid prokaryotic and vertebrate adaptive immune systems. *Science* **353**, aaf8729 (2016).
30. K. Blin, W. Wohlleben, T. Weber, Patscanui: An intuitive web interface for searching patterns in DNA and protein data. *Nucleic Acids Res.* **46**, W205–W208 (2018).
31. G. Saraconi, F. Severi, C. Sala, G. Mattiuz, S. G. Conticello, The RNA editing enzyme APOBEC1 induces somatic mutations and a compatible mutational signature is present in esophageal adenocarcinomas. *Genome Biol.* **15**, 417 (2014).
32. E. Zuo *et al*., Cytosine base editor generates substantial off-target single-nucleotide variants in mouse embryos. *Science* **364**, 289–292 (2019).
33. S. Jin *et al*., Cytosine, but not adenine, base editors induce genome-wide off-target mutations in rice. *Science* **364**, 292–295 (2019).
34. Y. Tong *et al*., Highly efficient DSB-free base editing for streptomycetes with CRISPR-BEST. National Center for Biotechnology Information. https://www.ncbi.nlm.nih.gov/bioproject/557658. Deposited 31 July 2019.
35. D. E. Deatherage, J. E. Barrick, Identification of mutations in laboratory-evolved microbes from next-generation sequencing data using breseq. *Methods Mol. Biol.* **1151**, 165–188 (2014).
36. S. D. Bentley *et al*., Complete genome sequence of the model actinomycete *Streptomyces coelicolor* A3(2). *Nature* **417**, 141–147 (2002).
37. K. L. Cox, R. H. Baltz, Restriction of bacteriophage plaque formation in *Streptomyces* spp. *J. Bacteriol.* **159**, 499–504 (1984).
38. M. A. Richardson, S. Kuhstoss, P. Solenberg, N. A. Schaus, R. N. Rao, A new shuttle cosmid vector, pKC505, for streptomycetes: Its use in the cloning of three different spiramycin-resistance genes from a *Streptomyces ambofaciens* library. *Gene* **61**, 231–241 (1987).
39. J. K. Epp, S. G. Burgett, B. E. Schoner, Cloning and nucleotide sequence of a carbomycin-resistance gene from *Streptomyces thermotolerans*. *Gene* **53**, 73–83 (1987).
40. V. A. Birmingham *et al*., Cloning and expression of a tylosin resistance gene from a tylosin-producing strain of Streptomyces fradiae. *Mol. Gen. Genet.* **204**, 532–539 (1986).
41. K. Blin *et al*., antiSMASH 5.0: Updates to the secondary metabolite genome mining pipeline. *Nucleic Acids Res.* **47**, W81–W87 (2019).
42. C. Rückert *et al*., Complete genome sequence of the kirromycin producer *Streptomyces collinus* Tü 365 consisting of a linear chromosome and two linear plasmids. *J. Biotechnol.* **168**, 739–740 (2013).
43. U. Dähn *et al*., Stoffwechselprodukte von mikroorganismen. 154. Mitteilung. Nikkomycin, ein neuer hemmstoff der chitinsynthese bei pilzen. *Arch. Microbiol.* **107**, 143–160 (1976).
44. D. Iftime *et al*., Identification and activation of novel biosynthetic gene clusters by genome mining in the kirromycin producer *Streptomyces collinus* Tü 365. *J. Ind. Microbiol. Biotechnol.* **43**, 277–291 (2016).
45. E. M. Musiol-Kroll *et al*., Polyketide bioderivatization using the promiscuous acyltransferase KirCII. *ACS Synth. Biol.* **6**, 421–427 (2017).
46. H. L. Robertsen *et al*., Filling the gaps in the kirromycin biosynthesis: Deciphering the role of genes involved in ethylmalonyl-CoA supply and tailoring reactions. *Sci. Rep.* **8**, 3230 (2018).
47. R. E. Haurwitz, M. Jinek, B. Wiedenheft, K. Zhou, J. A. Doudna, Sequence- and structure-specific RNA processing by a CRISPR endonuclease. *Science* **329**, 1355–1358 (2010).
48. O. Genilloud, Mining actinomycetes for novel antibiotics in the omics era: Are we ready to exploit this new paradigm? *Antibiotics (Basel)* **7**, 85 (2018).
49. J. Stonesifer, R. H. Baltz, Mutagenic DNA repair in *Streptomyces*. *Proc. Natl. Acad. Sci. U.S.A.* **82**, 1180–1183 (1985).
50. C. S. Nabel *et al*., AID/APOBEC deaminases disfavor modified cytosines implicated in DNA demethylation. *Nat. Chem. Biol.* **8**, 751–758 (2012).